Journal of Building Engineering 76 (2023) 107043

Contents lists available at ScienceDirect

Journal of Building Engineering

journal homepage: www.elsevier.com/locate/jobe

Magnesium phosphate cement incorporating sheep wool fibre for thermal insulation applications

A. Maldonado-Alameda, A. Alfocea-Roig, S. Huete-Hernández, J. Giro-Paloma, J.M. Chimenos, J. Formosa *

Department de Ciència de Materials I Química Física, Universitat de Barcelona, C/ Martí I Franquès, 1-11, 08028, Barcelona, Spain

ARTICLE INFO

Keywords:
Magnesium phosphate cement
Low-grade magnesium oxide
By-product
Valorisation
Sheep wool fibre
Design of experiments

ABSTRACT

The increasing use of synthetic fibres in clothing and the high quality of sheep wool fibre (SWF) from the Australian and New Zealand market leads to a decline in the interest in SWFs produced in European countries, considering them as waste that could be valorised within the framework of a circular economy. The use of natural fibre in cement-based composites presents the main issue of durability due to the alkaline pH media of conventional cement. The use of a low-pH cement could improve the viability of combining natural fibres in this low-pH cement as matrix for developing composites. One of these low-pH cements is magnesium phosphate cement (MPC). As a ceramic material the MPC presents high thermal conductivity (~1 W m^{-1} K^{-1}) to be used as isolating material. The present work combines MPC formulated with an industrial by-product (low-grade magnesium oxide; LG-MgO) and Spanish SWF, to develop new sustainable cement-based materials (Sust-MPC-SWF) for thermal building insulation applications. The physical, thermal, and mechanical properties of Sust-MPC-SWF were evaluated to determine the optimal formulation through a design of experiments (DoE). Thirteen formulations designed by DoE were conducted with different sheep wool fibre/cement (SWF/C) and sheep wool fibre/extra water (SWF/EW) ratios. A statistical model was obtained and the optimal formulation (SWF/C = 0.36 and SWF/EW = 0.25) was validated. The increase in SWF content led to an enhancement of thermal and acoustic insulation properties of Sust-MPC-SWF, with similar results to other building materials commercialized with these features.

1. Introduction

There is an undeniable fact that climate change and energy demand are the main threats facing society and planet earth in the coming decades [1,2]. Many industrial and urban activities require complex processes which consume a high amount of energy and carbon dioxide (CO_2) emissions. These processes contribute to the gradual increase in the planet's average annual temperature due to the greenhouse effect, leading to severe environmental problems [3]. In this sense, the building field is one of the highest-polluting industrial sectors due to its carbon and energy-intensive activities and manufacturing processes [4].

On the one hand, among the most polluting industries encompassed in this sector is the cement industry [5,6]. Ordinary Portland cement (OPC) is the most worldwide produced material due to its cost, availability, and mechanical properties. Nowadays, the global production capacity of OPC is more than 4100 Mt per year [7]. OPC industry is currently the third-largest industrial energy consumer

* Corresponding author.
E-mail address: joanformosa@ub.edu (J. Formosa).

https://doi.org/10.1016/j.jobe.2023.107043
Received 4 April 2023; Received in revised form 31 May 2023; Accepted 7 June 2023
Available online 14 June 2023

and the second-largest industrial CO_2 emitter globally [8]. For this reason, the OPC industry is increasingly striving to minimise its impact on the environment and the population [9]. The current solutions focus on improving resource and energy efficiency and the development of novel binders based on low carbon manufacturing [10]. Accordingly, new alternative binders have emerged in recent years, extending their application range in diverse technology areas [11]. These alternative cements can contribute to the EU 2050 strategic policy, based on a low-carbon economy, circular economy, and efficiency in using natural resources and energy [12,13].

On the other hand, buildings are responsible for 40% of global CO_2 emissions [14] and consume approximately 40% of global primary energy [15], mainly due to the use of heating, ventilating, and air conditioning (HVAC) systems to provide thermal comfort in both residential and non-residential buildings [16]. For this reason, the search for solutions to the minimisation of energy consumption in buildings becomes crucial to mitigate local and global climate change [17]. In this sense, the EU is recasting its regulations for energy performance in buildings, aiming to promote the building sector decarbonisation and move towards zero-emission building development [18]. Finally, from a materials engineering perspective, it is important to continue developing alternative insulation materials, which can contribute to energy savings in buildings [19].

In this context, this research approaches the development of new sustainable cement-based materials to reduce the use of the OPC as a building material and favour the energy efficiency of buildings. Concretely, this work formulates magnesium phosphate cement (MPC) incorporating sheep wool fibre (SWF) to enhance its thermal insulation properties and decrease energy consumption in buildings. MPC is an acid-base cement being part of the family of Chemically Bonded Phosphate Ceramics (CBPCs) [20]. Its manufacturing presents ecological and environmental benefits compared with OPC manufacturing [21]. MPC offers numerous advantages, including excellent biocompatibility, fast setting, and high early strength, which allow its application as a rapid repair material, hazardous and toxic waste stabiliser, and biomedical material [22]. Moreover, the neutral pH of MPCs cementitious matrixes can be interesting to incorporate natural fibres [23,24] compared to OPC (pH ~ 12–13) since high alkalinity leads to the degradation of the fibres [25]. Regarding SWF, the increasing use of synthetic fibres in clothing and low-quality wool led to a decline in the commercial interest and value of SWF produced in European countries [26]. Nowadays, SWF generates high expenses for the farms and the administrations since it is classified as special waste because it needs a sterilisation treatment to remove pathogenic organisms before its disposal [27]. For this reason, the scientific community are seeking alternatives to valorise this residue in other production sectors such as the building and construction fields. One of these alternatives is the incorporation of SWF in cement-based materials [28]. Most of the studies in the literature incorporate SWF in an OPC matrix to assess their thermal and mechanical properties. SWF stand out for its thermal and acoustic insulation properties, non-flammability and non-toxicity, and the possibility of enhancing the bending properties of cement-based materials [29]. The obtained results generally demonstrated a substantial enhancement of thermal insulation. However, the alkalinity of the cement matrix implies the degradation of SWF, which leads to a decrease in mechanical performance [27,29,30]. In this sense, using a neutral cement-based matrix such as MPC could enhance the final properties of SWF cement composites.

This study aimed to assess the potential use of MPC and SWF to develop a new sustainable insulation material to maintain thermal comfort in buildings. The originality of this work mainly lies in the incorporation of SWF in an alternative cement-based material with a lower pH than OPC. In addition, a low-grade magnesium oxide (LG-MgO) was used to formulate a more sustainable MPC (Sust-MPC) with a lower CO_2 footprint [31]. Hence, this is the first time that SWFs are used in this kind of matrix, MPC and/or Sust-MPC, for developing a composite material. In a previous study conducted by the authors the lowest thermal conductivity achieved with Sust-MPC formulation as a function of W/C ratio and a setting retardant additive was 0.89 W m^{-1} K^{-1} [32]. The present investigation evaluated Sust-MPC-SWF properties as a function of sheep wool fibre/cement (SWF/C) and sheep wool fibre/extra water (SWF/EW) ratios using a design of experiments (DoE). Thermal, physical, and mechanical properties were determined and then evaluated through the analysis of variance (ANOVA) to determine the optimal formulation for its use as a passive thermal panel.

2. Experimental procedure

2.1. Materials

The LG-MgO was provided by Magnesitas Navarras, S.A. company (Navarra, Spain). This by-product is generated during the calcination of natural magnesite ($MgCO_3$) to produce magnesia (MgO). Furthermore, the food-grade monopotassium phosphate (MKP) was supplied by J. Norken S.L. (Barcelona, Spain). This phosphate source is commonly used as fertiliser and has a purity of 99.8%. The authors previously reported the characterisation of LG-MgO and MKP [33,34]. The SWF used in this research proceeds from the Spanish production of sheep wool, which is considered a residue of the livestock industry due to its low interest. This research aims to modify the Sust-MPC thermal and acoustic properties by incorporating natural fibres, which offer excellent thermal and acoustic insulation [35,36]. For this purpose, the fibres were previously washed and then minced (<5 mm) with a mincer machine (Moulinex A320R1) to favour the mix with MPC paste.

2.2. Design of experiments: optimal formulation

Design of Experiments (DoE) is an efficient method that allows designing a material's ideal dosage, which depends on several factors and restrictions, using the minimum number of experiments or tests [32]. The present research used a response surface methodology (RSM) with a quadratic design to determine optimal formulation using previously obtained results. RSM allowed generating of a response surface plot calculated from statistical polynomic equations derived from the obtained results. Each surface plot represents the results obtained for each evaluated property (response) of the Sust-MPC-SWF. Thermal conductivity, apparent density, modulus of elasticity (MOE), and flexural strength were the responses evaluated to obtain the optimal Sust-MPC-SWF formulation. LG-MgO and MKP to cement (LG-MgO/C and MKP/C) ratios were kept constant in all the experiments, consisting of

Table 1
DoE formulations, fixed ratios and variable factors.

Run	Formulations	Fixed ratios			Variable Factors	
		LG-MgO/*C*	*MKP/C*	*W/C*	*SWF/C*	*SWF/EW*
1	30SWF-25 E W	0.6	0.4	0.4	0.30	0.25
2	20SWF-20 E W	0.6	0.4	0.4	0.20	0.20
3	30SWF-32 E W	0.6	0.4	0.4	0.30	0.32
4	16SWF-25 E W	0.6	0.4	0.4	0.16	0.25
5	20SWF-30 E W	0.6	0.4	0.4	0.20	0.30
6	30SWF-25 E W	0.6	0.4	0.4	0.30	0.25
7	30SWF-25 E W	0.6	0.4	0.4	0.30	0.25
8	30SWF-18 E W	0.6	0.4	0.4	0.30	0.18
9	40SWF-20 E W	0.6	0.4	0.4	0.40	0.20
10	30SWF-25 E W	0.6	0.4	0.4	0.30	0.25
11	44SWF-25 E W	0.6	0.4	0.4	0.44	0.25
12	30SWF-25 E W	0.6	0.4	0.4	0.30	0.25
13	40SWF-30 E W	0.6	0.4	0.4	0.40	0.30

Table 2
Step-by-step procedure for Sust-MPC-SWF formulation.

Stages	Time (s)
Precursors and kneading water addition	0
Mixing start	1
Stop mixing + wool addition	120
Mixing	130
Stop mixing + extra water addition	190
Mixing	200
Stop mixing + wool addition	260
Mixing	270
Stop mixing + pouring	360
Compaction	370
Curing	970

0.6 and 0.4, respectively. The water/cement (W/C) ratio was fixed at 0.4. Two variable factors were considered. On the one hand, the sheep wool fibre/cement (SWF/C) ratio was fixed between 0.2 and 0.4. On the other hand, the sheep wool fibre/extra water (SWF/EW) ratio was fixed between 0.2 and 0.3. SWF was used dried in order to facilitate the study and to avoid a lack of consistency in the results. As it is well known SWF adsorbs part of the kneading water, hence extra water is needed for obtaining the proper workability in the range of study. Hence, both ranges were selected by conducting a preliminary study taking into account the workability during the mixture with a planetary mixer for mortars as well as the final aspect of the product. Table 1 summarises the formulations under study, where the fixed ratios were the same for all the formulations meanwhile the effect of the variable factors were evaluated by means of the software (Design Expert®). The ratios and the statistical approach were conducted by following the methodology reported in previous studies published by the authors [32,37].

Once measured and analysed the obtained responses (thermal conductivity, apparent density, modulus of elasticity (MOE), and flexural strength) for each run, the optimal formulation is determined through a statistical model, assigning the constraints (goals and importance) of each variable factor and response studied. Finally, the preparation of the optimal formulation is performed to validate the feasibility of DoE.

2.3. Sust-MPC-SWF preparation

The preparation of Sust-MPC-SWF was performed through a strict protocol to avoid possible errors and changes caused by the complexity of the preparation process, which could directly affect their final properties. SWF was previously washed, dried in an oven at 60 °C for 24 h and then minced with a mincer machine. Table 2 summarises the chronology steps for the formulation of Sust-MPC-SWF samples and the time when the corresponding stage starts. Before the mixing process, the solid cement components (LG-MgO and MKP) must be weighed and homogenised in the mortar planetary mixer for 1 min. The preparation process starts when the first drop of water contacts the homogenised solids (time 0). Then, i) solids binder precursors (LG-MgO and MKP) and kneading water are mixed for 120 s. Subsequently, ii) half of the SWFs are added and mixed for 60 s. Afterwards, iii) extra water is added and mixed for 60 s. iv) The other half of the SWFs are added and mixed for 90 s. Finally, the fresh Sust-MPC-SWF paste is poured into plate-shaped (150 × 150 × 50 or 300 × 300 × 30 mm) wood moulds and then pressed (for 10 min) in a universal compression test machine until the sample reaches 30 mm of thickness. Then the specimens are cured at laboratory conditions (23 °C ± 2 °C and 50% ± 5% relative humidity) for 24 h.

After 24 h of curing, the specimens are demoulded and dried at 40 °C for three days to remove the “free water” in Sust-MPC-SWF. Finally, the specimens are placed in a container with silica gel until the experimental trials to avoid humidity absorption by the SWF. Fig. 1 depicts the final appearance of Sust-MPC-SWF specimens.

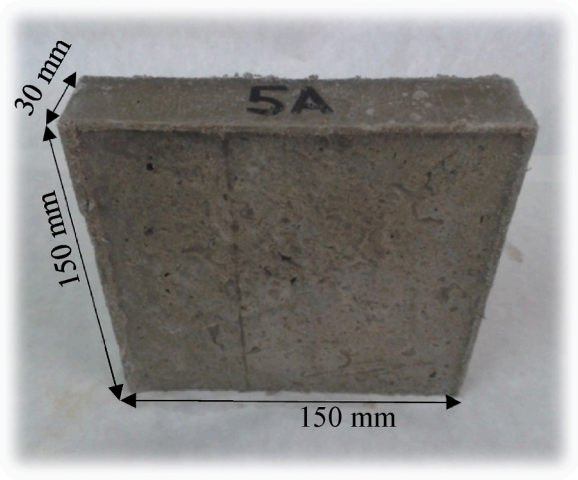

Fig. 1. Final appearance of Sust-MPC-SWF specimen.

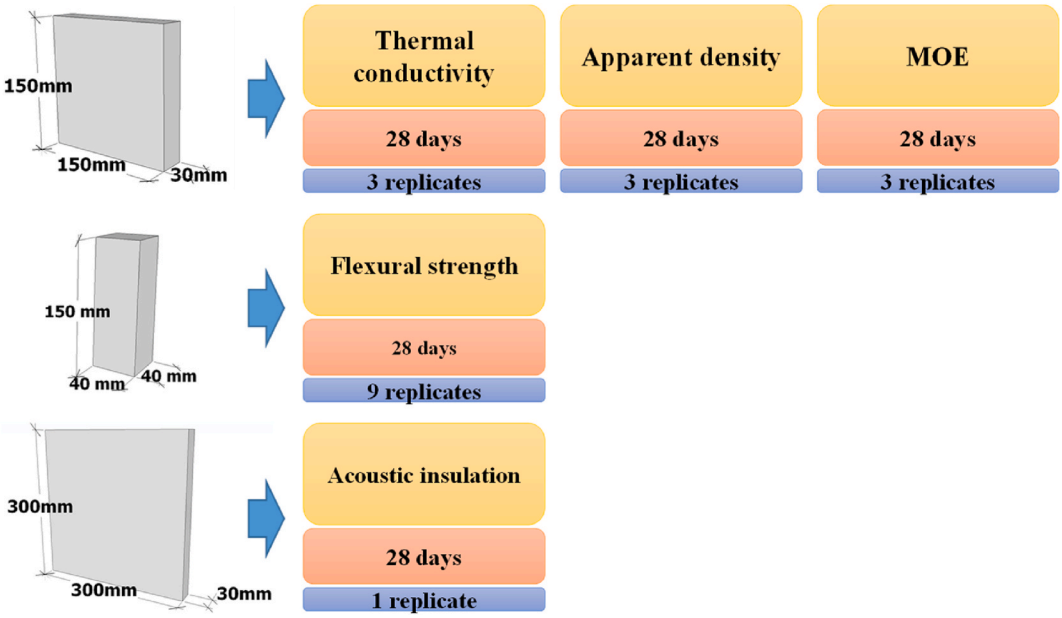

Fig. 2. Flowsheet of the experimental trials.

2.4. Property measurements

Fig. 2 shows the flowsheet of the experimental trials conducted. The property measurements were carried out using different-shaped specimens. The plate-shaped specimens of 150 × 150 × 30 mm were used to evaluate the thermal conductivity (λ), apparent density (ρ), and Modulus of Elasticity (MOE), while the prismatic-shaped specimens (150 × 40 × 40 mm) were used to determine the flexural strength (σ). Finally, the largest plate-shaped specimen (300 × 300 × 30 mm) was performed just for the proposed optimal formulation to assess the acoustic insulation. The properties considered in the statistical study were thermal conductivity (λ), apparent density (ρ), Modulus of Elasticity (MOE), and flexural strength (σ), while acoustic insulation was just evaluated for the proposed optimal formulation.

2.4.1. Thermal conductivity (λ)

Thermal conductivity was measured using Quickline™-30, Anter Corporation (USA), equipment. The equipment follows a dynamic measurement method based on the ASTM D5930 standard to determine thermal conductivity [38]. Two surface probes with a measuring range of 0.01–0.3 W m^{-1} K^{-1} and 0.3–2.0 W m^{-1} K^{-1} were used. During samples measurements, the ambient temperature was 23.0 °C ± 2.0 °C, and the relative humidity was 50% ± 5%. The thermal conductivities of each plate-shaped specimen (150 × 150 × 30 mm) were computed from two measured values. This thermal property allowed assessing the effect of wool content on the

Table 3
Responses of the DoE.

Formulations	Responses			
	λ ($W{\cdot}m^{-1}{\cdot}K^{-1}$)	ρ ($kg{\cdot}m^{-3}$)	MoE (GPa)	σ (MPa)
30SWF-25 E W	0.152	830	0.24	0.31
20SWF-20 E W	0.173	905	0.62	1.01
30SWF-32 E W	0.216	993	0.67	2.54
16SWF-25 E W	0.209	1015	0.88	2.01
20SWF-30 E W	0.227	1050	0.97	2.68
30SWF-25 E W	0.140	840	0.24	0.46
30SWF-25 E W	0.141	820	0.24	0.33
30SWF-18 E W	0.189	876	0.43	1.78
40SWF-20 E W	0.154	813	0.20	1.99
30SWF-25 E W	0.140	850	0.22	0.45
44SWF-25 E W	0.164	833	0.18	2.19
30SWF-25 E W	0.160	860	0.24	0.77
40SWF-30 E W	0.157	850	0.28	1.51

thermal behaviour of Sust-MPC-SWF.

2.4.2. Bulk density (ρ)

The plate-shaped specimens used for the thermal conductivity test were previously conditioned to measure the bulk density, which was determined by weighing and measuring each specimen. The sample dimensions were computed from the average thickness, width, and length (8 measures per dimension).

2.4.3. Modulus of elasticity (MoE)

Modulus of Elasticity (MoE) was determined using an ultrasonic pulse velocity tester (C368, Matest, Italy) following the UNE-EN 12504-4 standard. The equipment consisted of an emitter transducer (T_x) and a receiver transducer (R_x) operating at 50 Hz. The emitter applies an acoustic wave transmitted throughout the thickness of each plate-shaped specimen. Then, the receiver detects the wave signal, and the equipment can measure the delay time. MoE was calculated (five measurements per specimen) through Eqs. (1) and (2):

$$MoE = \rho \cdot V^2 \quad \text{Eq. 1}$$

$$V = 2 \cdot T \cdot f \quad \text{Eq. 2}$$

where ρ ($kg{\cdot}m^{-3}$) is the bulk density, V ($m{\cdot}s^{-1}$) is the wave passage velocity, T (m) is the thickness of the specimen, and f (Hz) is the vibration frequency.

2.4.4. Flexural strength (σ)

The flexural strength measurement was carried out using technical equipment (Zmart-PRO, ZwickRoell, Germany) following the standard UNE-EN 196-1 method. The plate-shaped specimens (150 × 150 × 30 mm) used in the previously described tests were cut to obtain three prism-shaped specimens (40 × 40 × 150 mm) using a cutting machine. A progressive load until fracture was applied with a loading rate of 10 mm min^{-1}. Flexural strength was computed by nine specimens of each formulation using Eq. (3):

$$Flexural\ strength = \frac{1.5 \cdot F \cdot L}{b \cdot h^2} \quad \text{Eq. 3}$$

where F is the maximum load applied, L is the distance between the two support rods, b is the length of the specimen, and h *is* the height of the prism-shaped specimen.

2.4.5. Sound reduction index

The acoustic insulation level was evaluated through a standardized test according to the UNE-EN 140–1. Two interconnected cabins with a square hole of 300 × 300 mm were used. The largest plate-shaped specimen (300 × 300 × 30 mm) was placed in the square hole. A loudspeaker (noise emitter) was placed in one of the cabins. Two microphones were placed in each cabin to obtain the emission (Le) and immission (Lr) levels. The microphones (MI 17 type of ¼'') allow recording the decibel data at different frequencies (20 Hz-4kHz (±0.5 dB); 4–20 kHz (±1 dB)) to compare the noise level between the two cabins and thus obtain the sound reduction index [39]. The data acquisition was recorded with the help of a DA-20 equipment and DA-20PA1 v2.0 software from RION Co., Ltd. In this case, the test was only performed on the optimal formulation and a MPC without sheep wool fibre as reference material.

3. Results and discussion

3.1. DoE: analysis of responses

The DoE analysis is based on the analysis of variance (ANOVA) to predict an optimal response. The p-value allows interpretation of the obtained results. This parameter represents the lowest level of significance that would lead to rejection of the null hypothesis,

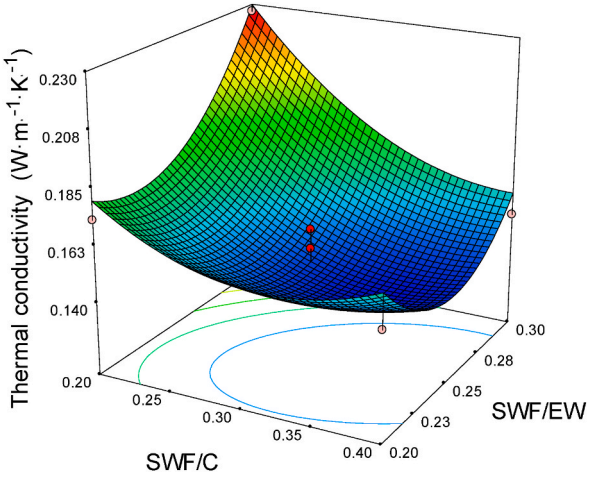

Fig. 3. Surface plot of the thermal conductivity.

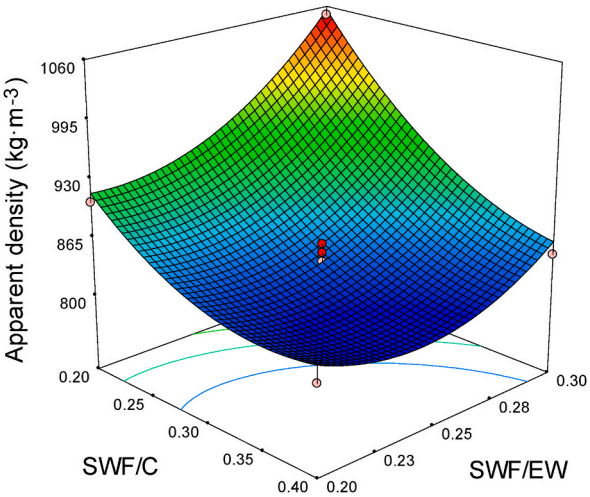

Fig. 4. Surface plot of the bulk density.

indicating that the controllable factor does not affect the response under study. Therefore, this factor will be statistically significant with a confidence level above 95% if the p-value is smaller than 0.05. The DoE was significant for all the responses analysed in the present study. Table 3 summarises the experimental values obtained for each response. All the equations of the statistical model were mathematically fitted. Thus, each response analysed allowed for determining a mathematical formula, which adjusted to the response surface. The following sub-sections discuss and present the proposed models (in terms of actual factors) for each response under study.

3.1.1. Thermal conductivity (λ)

Thermal conductivity (λ) is an important parameter to determine the thermal insulation capability of a construction material [40]. Therefore, the main goal of this investigation was to minimise thermal conductivity through the incorporation of SWF (Table 3). As a result of formulations proposed by DoE, the lowest thermal conductivity was 0.140 W m^{-1} K^{-1} in the 30SWF-25 E W formulation, while the highest was 0.227 W m^{-1} K^{-1} in the 20SWF-30 E W formulation (Table 3). The experimental values of the thermal conductivity allowed determining the mathematical model (Eq. (4)) and the surface plot (Fig. 3). The model presented a standard deviation and an R^2 value of 0.01 and 0.91, respectively. Focusing on the surface plot of thermal conductivity depending on variable factors studied (Fig. 3), the authors expected a linear trend based on the decrease in thermal conductivity when increase the amount of SWF fibres and vice-versa. However, the minimum thermal conductivity is around the median value of SWF/C (0.3) and SWF/EW (0.25) ranges. This fact agrees with the quadratic adjustment presented by both variable factors shown in Eq. (4) and reveals that both the increase and decrease in EW negatively affect the objective of minimising thermal conductivity. On the one hand, a lower EW content leads to less evaporation of "free water" during the curing process of Sust-MPC-SWF, generating less porosity and increasing thermal conductivity [32]. On the other hand, the unexpected increase in thermal conductivity as increased EW content is probably due to the high hygroscopicity of SWF [27], which leads to moisture trapping and the consequent increase in thermal conductivity as

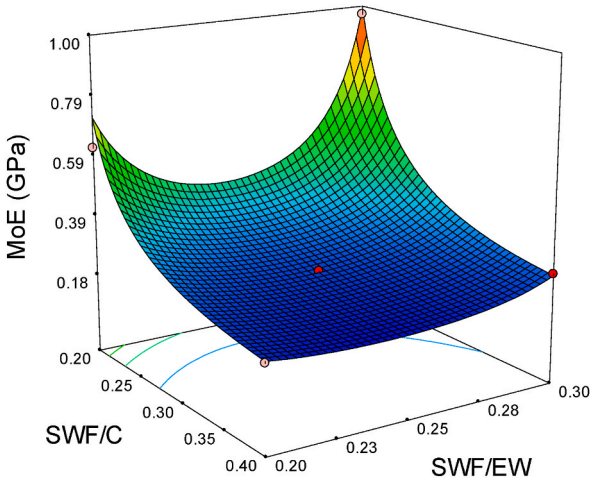

Fig. 5. Surface plot of the MoE.

reported elsewhere [41]. However, it could also be due to the high compaction of SWF during the sample preparation [42]. The excess of water favours the compaction of SWF, reducing their voids and leading to an increase in the thermal conductivity.

$$\lambda\left(\frac{W}{m\cdot K}\right)=0.69-0.50\cdot\frac{SWF}{C}-3.75\cdot\frac{SWF}{EW}-2.55\cdot\frac{SWF}{C}\cdot\frac{SWF}{EW}+1.58\cdot\left(\frac{SWF}{C}\right)^2+9.5\cdot\left(\frac{SWF}{EW}\right)^2 \quad \text{Eq. 4}$$

3.1.2. Bulk density (ρ)

The bulk density is significant in defining potential materials applications in the building field. Table 3 summarises bulk density responses, where the lowest (813 kg m^{-3}) was obtained in the 40SWF-20 E W formulation, while the highest (1050 kg m^{-3}) was in the 20SWF-30 E W formulation. The mathematical model of bulk density revealed a quadratic adjustment between the two variable factors (SWF/C and SWF/EW), as shown in Eq. (5). The standard deviation and R^2 values were 18.62 and 0.97, respectively. The bulk density surface plot (Fig. 4) tendency was similar to the thermal conductivity surface plot (Fig. 3). As expected, the higher the amount of the fibres, the lower the bulk density obtained since the SWF is less dense than the cement. In addition, the increase in EW leads to a decrease in bulk density due to the increase of porosity generated by the evaporation of "free water" during the sample curing [32]. However, as it occurred in thermal conductivity, the maximum SWF/C ratio and the minimum SWF/EW ratio slightly increased bulk density. This behaviour is attributable to the increase in humidity due to the hygroscopicity of SWF. The higher the SWF content, the higher the moisture trapped in the specimens. Therefore, the increase in humidity leads to an increase in bulk density due to the higher density of water compared SWF [36].

$$\rho\left(\frac{kg}{m^3}\right)=1.78-1.48\cdot\frac{SWF}{C}-5.74\cdot\frac{SWF}{EW}-5.42\cdot\frac{SWF}{C}\cdot\frac{SWF}{EW}+3.59\cdot\left(\frac{SWF}{C}\right)^2+16.47\cdot\left(\frac{SWF}{EW}\right)^2 \quad \text{Eq. 5}$$

3.1.3. Modulus of elasticity (MoE)

The material's density and stiffness are intimately related to MoE. Therefore, the authors expected that the increase in SWF would lead to a decrease in MoE of Sust-MPC-SWF formulations. As a result of analysing the formulations proposed by DoE, the lowest MoE (0.20 GPa) was obtained in the 40SWF-20 E W formulation, while the highest (0.97 GPa) in the 20SWF-30 E W formulation, as shown in Table 3. Eq. (6) shows the mathematical model for fitting the response values of the MoE. The standard deviation and R^2 values were 0.20 and 0.99, respectively. Fig. 5 represents the surface plot of the MoE, where it is observed that the maximum value is obtained when the amount of EW and SWF decreases, as expected. The decrease in EW implies a lower porosity in the MPC matrix, causing higher densification and, therefore, a higher MoE value. The surface plot also revealed that the lower the amount of the fibres, the stronger the influence of the extra water percentage in MoE. In this sense, the increase in MoE as the SWF/EW ratio decreases is probably due to the higher compaction of fibres, which leads to a densification of the material. In contrast, it is observed that the increase in fibre amount leads to MoE stabilised values, as evidenced by the plateau as the SWF/C ratio approaches 0.4.

$$MoE^{-1}(GPa)=-33.2+50.1\cdot\frac{SWF}{C}+229\cdot\frac{SWF}{EW}-42.3\cdot\frac{SWF}{C}\cdot\frac{SWF}{EW}-40.4\cdot\left(\frac{SWF}{C}\right)^2-449\cdot\left(\frac{SWF}{EW}\right)^2 \quad \text{Eq. 6}$$

3.1.4. Flexural strength (σ)

The flexural strength responses of Sust-MPC-SWF formulations are shown in Fig. 6. The minimum flexural strength was presented by the 30SWF-25 E W formulation (0.31 MPa) and the maximum by the 20SWF-30 E W (2.68 MPa) formulation. Eq. (7) shows the adjusted formula to obtain the flexural strength according to the selected SWF/C and SWF/EW ratios. The standard deviation and R^2 values were 0.23 and 0.96, respectively. Fig. 6 depicts the surface plot of the flexural strength. Two maximums can be considered in

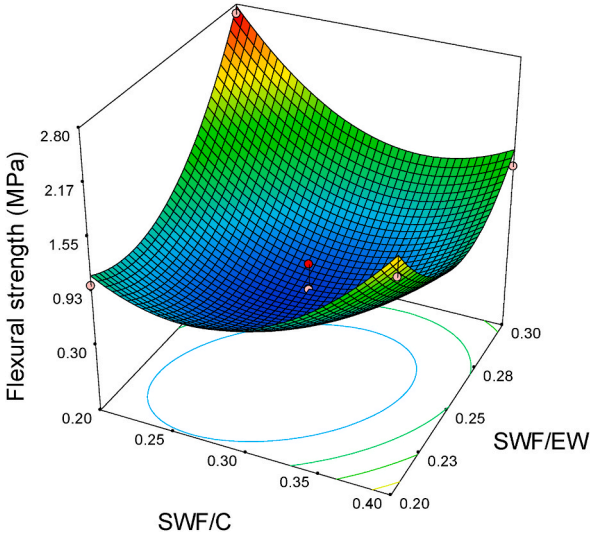

Fig. 6. Surface plot of the flexural strength.

Table 4
Optimisation criteria and optimal formulation.

Constraints			Predicted range		Optimal formulation	
Parameters	Goal	Importance	Lower	Upper	Experimental value	Predicted value
SWF/C	In the range	3	0.20	0.40	0.36	
SWF/EW	In the range	3	0.20	0.30	0.25	
λ ($W{\cdot}m^{-1}{\cdot}K^{-1}$)	Minimise	5	0.130	0.150	0.148	0.141
ρ ($kg{\cdot}m^{-3}$)	Minimise	5	791	829	818	810
MoE (GPa)	In the range	3	0.18	0.21	0.23	0.2
σ (MPa)	In the range	3	0.47	0.95	0.54	0.77

this parameter, one of them when the SWF and EW decrease and the other when these two factors increase. In the first case, the main reason is the lower proportion of EW and SWF, which reduces the porosity, causing a higher stiffness and enhancing the mechanical performance. The second case is due to the higher proportion of SWF since fibres act as a reinforcement of the cement matrix, enhancing flexural capacity before reaching fracture.

$$\sigma(MPa) = 16.7 - 17.1 \cdot \frac{SWF}{C} - 115 \cdot \frac{SWF}{EW} - 107.25 \cdot \frac{SWF}{C} \cdot \frac{SWF}{EW} + 73.5 \cdot \left(\frac{SWF}{C}\right)^2 + 306 \cdot \left(\frac{SWF}{EW}\right)^2 \quad \text{Eq. 7}$$

3.2. Optimal formulation

The optimal formulation (Table 4) was determined using the statistical models of each response presented above. However, as mentioned before, it was necessary to prepare the optimal formulation to validate the DoE, comparing the values obtained experimentally for each response with the values predicted by using the mathematical equations (Eq. 4-7). Moreover, considering that this research aimed to enhance the thermal properties of Sust-MPC-SWF for its use as a thermal passive construction system, the main goal was to minimise the thermal conductivity and bulk density (Table 4). The rest of the factors and responses were assigned within the range limits. Finally, the importance of each parameter was fixed at 3 (on a scale of 5), except thermal conductivity and bulk density, which were fixed at 5. Table 4 also shows that the statistical responses predicted by the mathematical model and the experimental responses values (thermal conductivity, bulk density, and flexural strength) matched, except for MoE. The difference in MoE may be due to the difference in laboratory temperature and humidity conditions during the curing of the DoE formulations shown in Table 1 and the optimal formulation (Table 4). The variation of these two parameters affects the densification of the material and, therefore, the stiffness. However, the MoE value is very close to the upper limit of the predicted value. Hence, it can conclude that DoE was performed successfully. Thermal conductivity, bulk density, and MoE of a Sust-MPC without SWF are 0.89 W m^{-1} K^{-1}, 1925.2 kg m^{-3}, and 16.50 GPa, respectively [32]. As it was expected thermal conductivity, bulk density, and MoE are significantly reduced when Sust-MPC-SWF are formulated in the proportions indicated in Table 4 and compared with previous works, (i.e.: 83.4%, 57.1%, and 98.6%, respectively).

3.2.1. Sound reduction index

Fig. 7a and b show the emission (Le) and immission (Li) noise levels of reference MPC and optimal formulation (36SWF-25 E W),

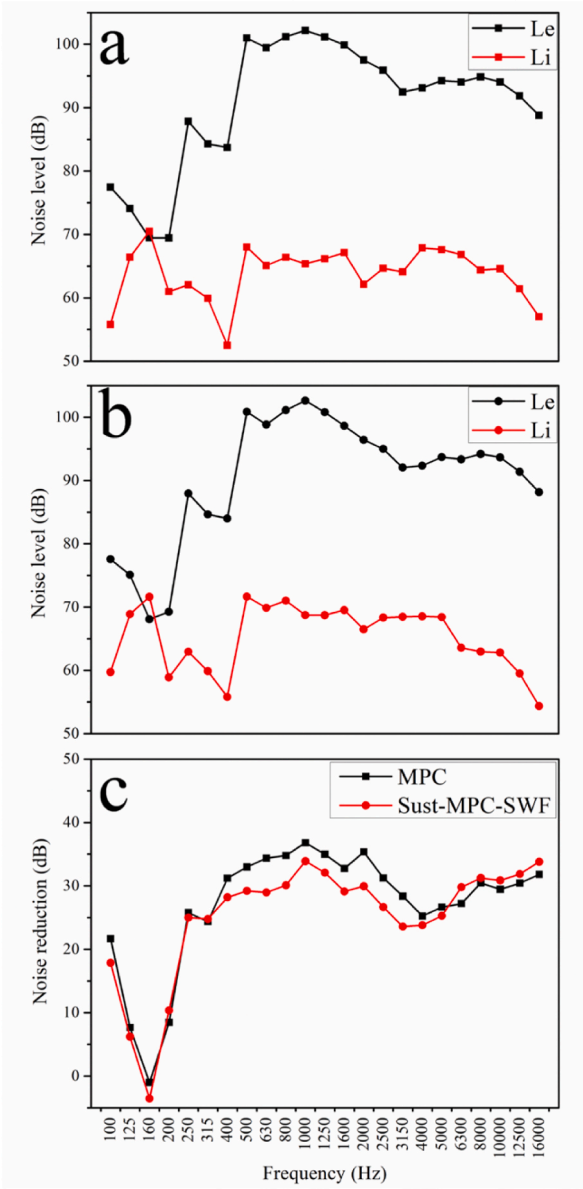

Fig. 7. (a) Emission and immission noise levels of reference MPC (b) Emission and immission noise levels of optimal formulation (c) Noise reduction achieved by reference MPC and optimal formulation.

respectively. A substantial reduction of level emissions in low, intermediate, and high frequencies can be observed, except in 120, 160, and 200 Hz. On the other hand, the sound reduction index in reference MPC is slightly higher than the optimal formulation, as shown in Fig. 7c. This fact is attributed to the difference in bulk density since the higher the density, the higher the acoustic insulation. In this sense, the reference MPC has a bulk density of around 1800 kg m^{-3}, as reported elsewhere [43]. Finally, it was demonstrated that the sound reduction index of the optimal formulation is similar to other materials such as wood wool and cellulose [29].

4. Conclusions

This research evidenced that it is possible to formulate a sustainable MPC with magnesium oxide by-product incorporating SWF as an admixture to improve thermal insulation properties (Sust-MPC-SWF). Furthermore, the formulation of Sust-MPC-SWF also promotes sustainability criteria using special waste and industrial by-products such as SWF and LG-MgO. In addition, Sust-MPC-SWF can contribute as potential insulation material in passive energy buildings to optimise energy efficiency and thermal comfort.

The DoE and the ANOVA statistical analysis allowed obtaining a model for further optimisation of Sust-MPC-SWF formulation, minimising thermal conductivity and apparent density. Therefore, the optimal dosage was obtained by considering mixing variables such as sheep wool fibres/cement (SWF/C) and sheep wool fibres/extra water (SWF/EW) ratios. The range, factors and responses

under study were appropriately adjusted to quadratic equations. The work demonstrated that it is possible to control the dosages by following the proposed methodology to diminish thermal conductivity and apparent density.

Both SWF/C and SWF/EW ratios evidenced a synergistic interaction as demonstrated in the surface plots of each response studied, where no linear trend is observed. The unexpected increase in thermal conductivity and apparent density in formulations with high fibre content is due to the hygroscopic nature of the SWF, leading to moisture absorption. The unexpected increase in MoE when the EW proportion increase is probably due to the high "free water" content, which favours the compaction of SWF and the densification of Sust-MPC-SWF. It was also revealed that SWF enhances the bending capacity when the SWF/EW ratio decrease.

The optimal formulation proposed a SWF/C ratio of 0.36 and a SWF/EW of 0.25. The experimental results obtained in this formulation validated the DoE performed in this investigation. The use of SWF for developing Sust-MPC-SWF allows to reduce of the thermal conductivity of Sust-MPC without SWF (83% of reduction for the optimal formulation), with a remarkable reduction of the mechanical properties. Considering the mechanical results of the optimal formulation, it would be concluded that the Sust-MPC-SWF composite could be used just as a non-structural material. For instance, it would be used a part for developing External Thermal Insulation Composite System (ETICS). Finally, the sound reduction index determined in the optimal formulation showed similar values to other building materials.

CRediT authorship contribution statement

A. Maldonado-Alameda: Data curation, Formal analysis, Investigation, Writing - original draft. **A. Alfocea-Roig**: Data curation, Formal analysis, Visualization, Writing - review & editing. **S. Huete-Hernández**: Resources, Visualization. **J. Giro-Paloma**: Visualization, Supervision, Writing - review & editing. **J. M. Chimenos**: Visualization, Supervision, Writing - review & editing, Funding acquisition. **J. Formosa**: Conceptualization, Visualization, Supervision, Methodology, Writing - review & editing, Funding acquisition.

Declaration of competing interest

The authors declare that they have no known competing financial interests or personal relationships that could have appeared to influence the work reported in this paper.

Data availability

Data will be made available on request.

Acknowledgements

This work is partially supported by Social Innova (FGB308411) company, by the Spanish Government with the Grant PID2021-125810OB-C21 funded by MCIN/AEI/10.13039/501,100,011,033 and by "ERDF A way of making Europe", and by the Catalan Government with the Grant 2021 SGR 00708. Furthermore, the Agència de Gestió d'Ajuts Universitaris i de Recerca (AGAUR) contributed through Ms A. Alfocea-Roig's PhD grant (FI-DGR 2021). The authors would like to thank Magnesitas Navarras, S.A. company for material supply. Dr. Jessica Giro-Paloma is a Serra Húnter Fellow.

References

[1] S.R. Paramati, U. Shahzad, B. Doğan, The role of environmental technology for energy demand and energy efficiency: evidence from OECD countries, Renew. Sustain. Energy Rev. 153 (2022), https://doi.org/10.1016/j.rser.2021.111735.
[2] D. Degroot, K. Anchukaitis, M. Bauch, J. Burnham, F. Carnegy, J. Cui, K. de Luna, P. Guzowski, G. Hambrecht, H. Huhtamaa, A. Izdebski, K. Kleemann, E. Moesswilde, N. Neupane, T. Newfield, Q. Pei, E. Xoplaki, N. Zappia, Towards a rigorous understanding of societal responses to climate change, Nature 591 (2021) 539–550, https://doi.org/10.1038/s41586-021-03190-2.
[3] L. Al-Ghussain, Global warming: review on driving forces and mitigation, Environ. Prog. Sustain. Energy 38 (2019) 13–21, https://doi.org/10.1002/ep.13041.
[4] E.W.L. Cheng, Y.H. Chiang, B.S. Tang, Exploring the economic impact of construction pollution by disaggregating the construction sector of the input-output table, Build. Environ. 41 (2006) 1940–1951, https://doi.org/10.1016/j.buildenv.2005.06.020.
[5] H.G. Van Oss, A.C. Padovani, Cement manufacture and the environment Part I: chemistry and technology, J. Ind. Ecol. 6 (2002) 89–105, https://doi.org/10.1162/108819802320971650.
[6] H.G. Van Oss, A.C. Padovani, Cement Manufacture and the Environment Part II: environmental Challenges and Opportunities Keywords alternative fuels carbon dioxide clinker greenhouse gases (GHG) industrial symbiosis portland cement, J. Ind. Ecol. 7 (2003) 93–126, https://doi.org/10.1162/108819803766729212.
[7] J.F. Reilly, Mineral commodity summaries 2020, Reston, VA. https://doi.org/10.3133/mcs2020, 2020.
[8] M.B. Ali, R. Saidur, M.S. Hossain, A review on emission analysis in cement industries, Renew. Sustain. Energy Rev. 15 (2011) 2252–2261, https://doi.org/10.1016/j.rser.2011.02.014.
[9] J. Lehne, F. Preston, Making Concrete Change: Innovation in Low-Carbon Cement and Concrete, 2018.
[10] I.E.A. International, E. Agency, Technology Roadmap for Cement, SpringerReference, 2011.
[11] M.C.G. Juenger, F. Winnefeld, J.L. Provis, J.H. Ideker, Advances in alternative cementitious binders, Cement Concr. Res. 41 (2011) 1232–1243, https://doi.org/10.1016/j.cemconres.2010.11.012.
[12] Institute for Sustainability Leadership, Industrial Transformation 2050 - Pathways to Net-Zero Emissions from EU Heavy Industry, 2019.
[13] P. Hoddinott, The Role of Cement in the 2050 Low Carbon Economy, 2013.
[14] A. Tallini, L. Cedola, A review of the properties of recycled and waste materials for energy refurbishment of existing buildings towards the requirements of NZEB, Energy Proc. 148 (2018) 868–875, https://doi.org/10.1016/j.egypro.2018.08.108.
[15] G. Martinopoulos, K.T. Papakostas, A.M. Papadopoulos, A comparative review of heating systems in EU countries, based on efficiency and fuel cost, Renew. Sustain. Energy Rev. 90 (2018) 687–699, https://doi.org/10.1016/j.rser.2018.03.060.
[16] Sholahudin Nasruddin, P. Satrio, T.M.I. Mahlia, N. Giannetti, K. Saito, Optimization of HVAC system energy consumption in a building using artificial neural network and multi-objective genetic algorithm, Sustain. Energy Technol. Assessments 35 (2019) 48–57, https://doi.org/10.1016/j.seta.2019.06.002.

[17] M. Santamouris, Innovating to zero the building sector in Europe: minimising the energy consumption, eradication of the energy poverty and mitigating the local climate change, Sol. Energy 128 (2016) 61–94, https://doi.org/10.1016/j.solener.2016.01.021.
[18] European Commission, DIRECTIVE of the EUROPEAN PARLIAMENT and of the COUNCIL on the Energy Performance of Buildings (Recast), European Union, 2021.
[19] B. Abu-Jdayil, A.H. Mourad, W. Hittini, M. Hassan, S. Hameedi, Traditional, state-of-the-art and renewable thermal building insulation materials: an overview, Construct. Build. Mater. 214 (2019) 709–735, https://doi.org/10.1016/j.conbuildmat.2019.04.102.
[20] A.S. Wagh, Introduction to Chemically Bonded Ceramics, in: E.S. Publishing (Ed.), Chem. Bond. Phosphate Ceram, Elsevier, 2016, pp. 1–16, https://doi.org/10.1016/B978-0-08-100380-0.00001-4.
[21] A.S. Wagh, Environmental Implications of Chemically Bonded Phosphate Ceramic Products, in: E.S. Publishing (Ed.), Chem. Bond. Phosphate Ceram, Elsevier, 2016, pp. 359–372, https://doi.org/10.1016/B978-0-08-100380-0.00020-8.
[22] M.A. Haque, B. Chen, Research progresses on magnesium phosphate cement: a review, Construct. Build. Mater. 211 (2019) 885–898, https://doi.org/10.1016/j.conbuildmat.2019.03.304.
[23] S. Manso, G. Mestres, M.P. Ginebra, N. De Belie, I. Segura, A. Aguado, Development of a low pH cementitious material to enlarge bioreactivity, Construct. Build. Mater. 54 (2014) 485–495, https://doi.org/10.1016/j.conbuildmat.2014.01.001.
[24] R. del Valle-Zermeño, J.E. Aubert, A. Laborel-Préneron, J. Formosa, J.M. Chimenos, Preliminary study of the mechanical and hygrothermal properties of hemp-magnesium phosphate cements, Construct. Build. Mater. 105 (2016) 62–68, https://doi.org/10.1016/j.conbuildmat.2015.12.081.
[25] J. Wei, C. Meyer, Degradation mechanisms of natural fiber in the matrix of cement composites, Cement Concr. Res. 73 (2015) 1–16, https://doi.org/10.1016/j.cemconres.2015.02.019.
[26] B. Petek, R. Marinšek Logar, Management of waste sheep wool as valuable organic substrate in European Union countries, J. Mater. Cycles Waste Manag. 23 (2021) 44–54, https://doi.org/10.1007/s10163-020-01121-3.
[27] M.C.M. Parlato, S.M.C. Porto, Organized framework of main possible applications of sheep wool fibers in building components, Sustain. Times 12 (2020), https://doi.org/10.3390/su12030761.
[28] R. Alyousef, H. Alabduljabbar, H. Mohammadhosseini, A.M. Mohamed, A. Siddika, F. Alrshoudi, A. Alaskar, Utilization of sheep wool as potential fibrous materials in the production of concrete composites, J. Build. Eng. 30 (2020), 101216, https://doi.org/10.1016/j.jobe.2020.101216.
[29] D. Jóźwiak-Niedźwiedzka, A.P. Fantilli, Wool-reinforced cement based composites, Materials 13 (2020), https://doi.org/10.3390/MA13163590.
[30] M.T. Marvila, H.A. Rocha, A.R.G. de Azevedo, H.A. Colorado, J.F. Zapata, C.M.F. Vieira, Use of natural vegetable fibers in cementitious composites: concepts and applications, Innov. Infrastruct. Solut. 6 (2021) 1–24, https://doi.org/10.1007/s41062-021-00551-8.
[31] R. del Valle-Zermeño, J. Giro-Paloma, J. Formosa, J.M. Chimenos, Low-grade magnesium oxide by-products for environmental solutions: characterization and geochemical performance, J. Geochem. Explor. 152 (2015), https://doi.org/10.1016/j.gexplo.2015.02.007.
[32] M. Niubó, J. Formosa, A. Maldonado-Alameda, R. del Valle-Zermeño, J.M. Chimenos, Magnesium phosphate cement formulated with low grade magnesium oxide with controlled porosity and low thermal conductivity as a function of admixture, Ceram. Int. 42 (2016), https://doi.org/10.1016/j.ceramint.2016.06.159.
[33] S. Huete-Hernández, A. Maldonado-Alameda, J. Giro-Paloma, J.M. Chimenos, J. Formosa, Fabrication of sustainable magnesium phosphate cement micromortar using design of experiments statistical modelling: valorization of ceramic-stone-porcelain containing waste as filler, Ceram. Int. 47 (2021) 10905–10917, https://doi.org/10.1016/j.ceramint.2020.12.210.
[34] S. Huete-hernández, A. Maldonado-alameda, A. Alfocea-roig, J. Giro-paloma, J.M. Chimenos, J. Formosa, Sustainable magnesium phosphate micromortars formulated with PAVAL ® alumina by-product as, Boletín La Soc. Española Cerámica y Vidr (2023) 1–15, https://doi.org/10.1016/j.bsecv.2023.02.001.
[35] T. Michael, S. Kumar, L. Kumar, M.P. Shettar, S. Pal, Materials Today : proceedings Assessing the potentials of Bamboo and sheep wool fiber as sustainable construction materials : a review, Mater. Today Proc. (2021), https://doi.org/10.1016/j.matpr.2021.05.322.
[36] O. Dénes, I. Florea, D.L. Manea, Utilization of sheep wool as a building material, Procedia Manuf. 32 (2019) 236–241, https://doi.org/10.1016/j.promfg.2019.02.208.
[37] J. Formosa, J.M. Chimenos, A.M. Lacasta, M. Niubó, Interaction between low-grade magnesium oxide and boric acid in chemically bonded phosphate ceramics formulation, Ceram. Int. 38 (2012) 2483–2493, https://doi.org/10.1016/j.ceramint.2011.11.017.
[38] A.H.-C. Shin, U. Kodide, Thermal conductivity of ternary mixtures for concrete pavements, Cem. Concr. Compos. 34 (2012) 575–582, https://doi.org/10.1016/j.cemconcomp.2011.11.009.
[39] R. del Rey, J. Alba, J.C. Rodríguez, L. Bertó, Characterization of new sustainable acoustic solutions in a reduced sized transmission chamber, Buildings 9 (2019), https://doi.org/10.3390/buildings9030060.
[40] L.D. Hung Anh, Z. Pásztory, An overview of factors influencing thermal conductivity of building insulation materials, J. Build. Eng. 44 (2021), https://doi.org/10.1016/j.jobe.2021.102604.
[41] D. Bosia, L. Savio, F. Thiebat, A. Patrucco, S. Fantucci, G. Piccablotto, D. Marino, Sheep wool for sustainable architecture, Energy Proc. 78 (2015) 315–320, https://doi.org/10.1016/j.egypro.2015.11.650.
[42] T.T. Nguyen, V. Picandet, P. Carre, T. Lecompte, S. Amziane, C. Baley, Effect of compaction on mechanical and thermal properties of hemp concrete, Eur. J. Environ. Civ. Eng. 14 (2010) 545–560, https://doi.org/10.1080/19648189.2010.9693246.
[43] A. Maldonado-Alameda, A.M. Lacasta, J. Giro-Paloma, J.M. Chimenos, L. Haurie, J. Formosa, Magnesium phosphate cements formulated with low grade magnesium oxide incorporating phase change materials for thermal energy storage, Construct. Build. Mater. 155 (2017) 209–216, https://doi.org/10.1016/j.conbuildmat.2017.07.227.